Adaptive Multi-Scale Gaussian-Laplacian Pyramid with Gabor Filtering for Microplastics Detection

Ahmad Cahyono Adi
Department of Computer Science and Electronics, Faculty of Mathematics and Natural Sciences, Universitas Gadjah Mada, Yogyakarta, Indonesia
ahmadcahyonoadi@mail.ugm.ac.id

Wahyono
Department of Computer Science and Electronics, Faculty of Mathematics and Natural Sciences, Universitas Gadjah Mada, Yogyakarta, Indonesia
wahyo@ugm.ac.id (corresponding author)

Received: 29 September 2025 | Revised: 16 November 2025 | Accepted: 21 November 2025

 DOI: https://doi.org/10.48084/etasr.15206

ABSTRACT

Microplastics, defined as plastic particles with characteristic dimensions smaller than 5 mm, have emerged as a major environmental pollutant, posing significant threats to marine ecosystems, wildlife, and human health. Accurate detection and classification of microplastics in environmental samples are therefore essential for monitoring their spatial distribution. This study proposes an adaptive Gaussian-Laplacian pyramid-based framework for multi-scale image decomposition to enhance microplastic detection in microscopic images. Unlike conventional methods that use a fixed number of pyramid levels, the proposed approach dynamically selects the most informative level for each image based on quantitative metrics such as variance, edge energy, and entropy. This adaptive selection ensures optimal feature extraction at the most relevant scale, improving detection accuracy for small and variably shaped microplastics. Detection is performed using a sliding window approach combined with a Support Vector Machine (SVM) classifier, followed by Non-Maximum Suppression (NMS) to eliminate duplicate detections. The system was evaluated on 574 microscopic images, achieving high detection sensitivity with an accuracy of 0.93 on Level 2 with a radius of 15 pixels. A comparative analysis with recent studies demonstrates that the proposed method offers superior scalability and balanced detection performance, particularly for small objects.

Keywords-microplastic detection; Gaussian-Laplacian pyramid; multi-scale image decomposition; contrast enhancement; object detection

I. INTRODUCTION

A significant environmental problem with plastic waste is that it gradually degrades into microplastics through physical abrasion, photodegradation, and chemical weathering processes [1-4]. These microplastic particles are highly resilient, persistent, and easily dispersed across air, soil, and water systems, which leads to their accumulation in various ecosystems. Moreover, once introduced into aquatic environments, microplastics can be ingested by marine organisms and subsequently transferred through the food chain, posing potential risks to human health, including inflammatory responses and potentially carcinogenic effects [1, 5].

In recent years, automated microplastic detection using computer vision techniques has attracted increasing attention for environmental monitoring [6], with deep learning approaches, such as Convolutional Neural Networks (CNNs), You Only Look Once (YOLO), and Mask Region-based CNN (R-CNN) demonstrating strong detection capabilities [7, 8]. However, these methods typically require large, well-annotated datasets, substantial computational resources, and long training times [9]. Moreover, microplastics are often very small in size and exhibit fine-grained textural variations and irregular boundaries that may be progressively attenuated or lost in deeper layers of convolutional feature hierarchies, leading to reduced sensitivity for micro-scale object detection [8, 10-13]. This limitation is particularly evident when such models are applied to datasets outside their original training domain. Therefore, such approaches have limited practical applicability in many laboratory and field settings, where sample diversity is high and manual annotation is time-consuming.

Additionally, classical machine learning classifiers such as Support Vector Machines (SVMs) and Random Forest while offering greater computational efficiency in this task, their

performance depends strongly on the discriminative power of the extracted features [14, 15].

To overcome these challenges, this study employs an adaptive multi-scale Gaussian-Laplacian pyramid model combined with Gabor filtering. In this framework, the Gaussian-Laplacian pyramid provides multi-resolution representations, and the proposed adaptive selection mechanism identifies the most informative pyramid level using statistical measures (variance, edge energy, and entropy) derived from Gabor-filtered responses. Gabor filtering enhances directional and texture characteristics relevant to microplastic structures. This adaptive strategy reduces unnecessary multi-scale operations and improves sensitivity to small and low-contrast microplastics. By relying on classical image processing and machine learning rather than large annotated datasets, the method remains practical for laboratory environments with limited computational resources.

II. PROPOSED METHOD

The complete workflow of the proposed adaptive multi-scale object detection framework based on a Gaussian-Laplacian pyramid enhanced with Gabor filtering and adaptive level selection is illustrated in Figure 1.

A. Dataset and Preprocessing

The experimental dataset used in this study was obtained from the Panats MP Project on Kaggle [16] and consists of 574 microscopic images. To reduce peripheral artifacts such as container edges and labels, a static cropping strategy is applied, retaining the central 30-85% of the image horizontally and 15-85% vertically. Then, the cropped images are resized to 1024 × 1024 pixels using bicubic interpolation to ensure consistent spatial resolution for multi-scale analysis based on Gaussian-Laplacian pyramid decomposition. As a single image may contain multiple microplastic particles, detection performance was evaluated at the object level. The dataset characteristics are summarized in Table I, and representative samples are shown in Figure 2.

TABLE I. DATA DESCRIPTION

Aspect	Description
Dataset Name	Microplastic Dataset
Static Crop	30-85% Horizontal Region, 15-85% Vertical Region
Total	574 Images containing 1,171 microplastic particles

B. Gaussian-Laplacian Pyramid Construction

In this work, the construction of the Gaussian and Laplacian pyramids follows established methodologies in multi-scale image analysis, as demonstrated in medical image fusion applications [17]. Firstly, the Gaussian pyramid is generated through iterative Gaussian blurring and downsampling, while the Laplacian pyramid captures high-frequency residuals between successive Gaussian levels, effectively isolating fine structural details critical for microplastic detection. After preprocessing, the next critical step in the pipeline involves constructing a Gaussian-Laplacian image pyramid.

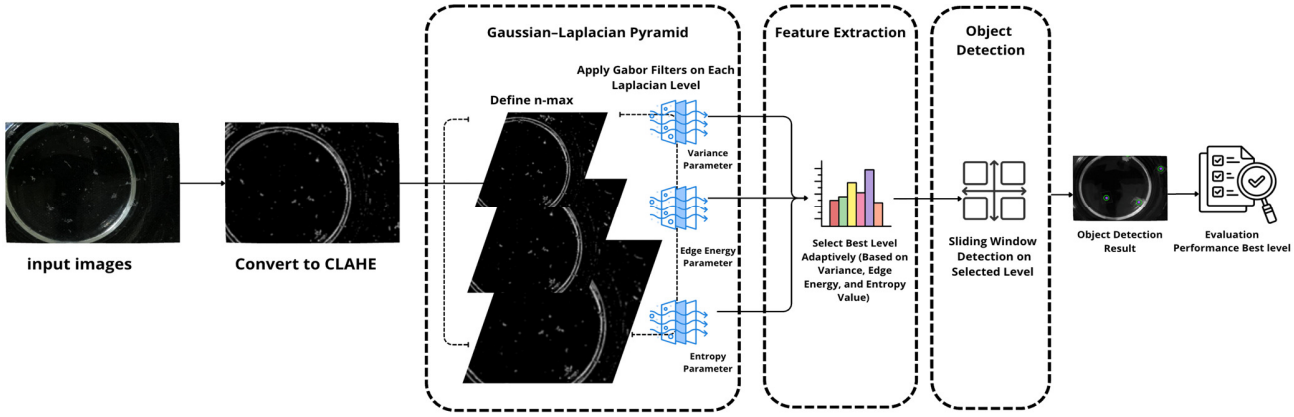

Fig. 1. Workflow of the proposed adaptive multi-scale Gaussian-Laplacian pyramid model.

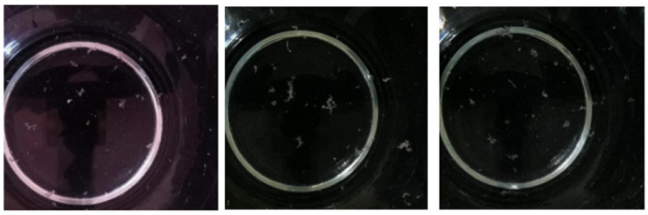

Fig. 2. Sample of microplastic dataset.

This multi-scale representation allows the algorithm to capture image features at various levels of detail, which is particularly important when detecting microplastics of varying shapes and sizes embedded in complex backgrounds. For each level l, a Gaussian-smoothed version of the image G_l is computed as:

$$G_l = G_{l-1} * K \quad (1)$$

where G_l refers to the image at level l of the pyramid, while G_{l-1} represents the image from the previous level. The K is the Gaussian kernel, typically a 5×5 or 7×7 matrix. This kernel is applied to the image through convolution, where each pixel is replaced by a weighted average of itself and its neighboring pixels, with the weights determined by the Gaussian distribution. This smoothing process helps in reducing high-

frequency noise and detail. In addition, the operation "$*$" denotes the convolution process, where a Gaussian kernel blurs the image before downsampling by a factor of 2 at each level, reducing resolution and capturing larger-scale features.

Then, the Laplacian pyramid isolates high-frequency details (e.g., edges, textures) by subtracting an upsampled Gaussian level from the current one, yielding the Laplacian layer L_i as:

$$L_i = G_i - G_{i+1} \quad (2)$$

G_{i+1} typically involves interpolation (e.g., bilinear) and may include Gaussian smoothing to prevent aliasing artifacts. The resulting Laplacian level L_l highlights the information lost during the downsampling from G_i to G_{i+1}, thus preserving fine structures such as microplastic edges. The pyramid is constructed up to six levels, with each level reducing the spatial resolution by half compared to the previous one. A visualization of the Gaussian-Laplacian pyramid is shown in Figure 3.

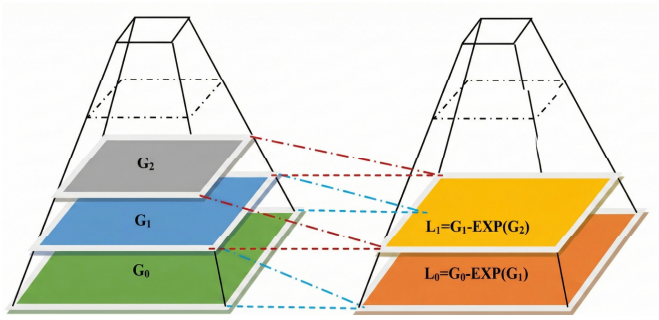

Fig. 3. Gaussian-Laplacian pyramid construction.

C. Adaptive Optimal Level Selection

While conventional pyramid-based approaches rely on fixed decomposition depths or processing all levels [17], the proposed method employs adaptive level selection to identify the most informative Laplacian pyramid level, improving both efficiency and detection accuracy. To achieve that, texture and structural characteristics are evaluated at each level to select the optimal scale.

Feature extraction is performed using Gabor filters and the Difference of Gaussian (DoG), including its anisotropic variant, which enhances edge information by suppressing low-frequency background components. Gabor filtering captures orientation- and frequency-specific texture responses through a multi-orientation and multi-scale filter bank defined as:

$$G(x, y, \theta, \lambda, \psi, \sigma, \gamma) = \exp\left(-\frac{x'^2+\gamma'^2 y'^2}{2\sigma^2}\right).cos\ (2\pi\frac{x'}{\lambda} + \psi) \quad (3)$$

where θ is the orientation, λ is the wavelength, ψ is the phase offset, σ is the standard deviation of the Gaussian envelope, γ is the spatial aspect ratio, and (x', y') are the rotated coordinates with respect to the filter orientation θ. In this work, the filter bank comprises 8 orientations ranging from 0° to 157.5° in steps of 22.5°, and three scales with wavelengths λ=4, 8, 16, ensuring sensitivity to a broad range of directional and frequency-specific patterns typical of microplastic structures.

Three statistical metrics are derived from the Gabor responses: variance, edge energy, and entropy to assess the informational content at each pyramid level. The variance measures intensity fluctuations, reflecting the presence of structured textures, and is defined as:

$$\sigma^2{}_l = \frac{1}{N}\sum_{i=1}^{N}(I_g\ (I) - \mu)^2 \quad (4)$$

where $I_g(i)$ denotes the Gabor response at pixel i, and μ is the mean intensity. The edge energy E_l quantifies the overall strength of edges by aggregating the gradient magnitudes and is calculated as:

$$E_l = \sum_i^n \left|\Delta\ i\ I_g(i)\right| \quad (5)$$

Moreover, entropy H_l is computed from the histogram of response intensities and captures the complexity and randomness of local textures:

$$H_l = -i\ \sum p(i) log_2\ p(i) \quad (6)$$

where $p(i)$ is the normalized histogram probability at intensity level i. These three metrics are then normalized and linearly combined into a single composite score S_l for each level:

$$S_l = \varpi_1\ .Norm\ (Var_l) + \varpi_2\ .Norm\ (E_l) + \varpi_3\ .Norm\ (H_l) \quad (7)$$

where ϖ_1, ϖ_2, ϖ_3 represent adjustable weights and $Norm$ indicates normalized values. The pyramid level i^* with the highest composite score is selected as the optimal scale for further processing:

$$i^* = \arg\max S_l \quad (8)$$

By isolating the level exhibiting the most discriminative texture, edge, and entropy characteristics, this adaptive selection mechanism ensures that the subsequent stages of contrast enhancement, feature filtering, and object detection are focused on the level most likely to contain salient microplastic features.

D. Contrast and Feature Enhancement

After identifying the optimal pyramid level(s), the algorithm performs binary thresholding on the contrast-enhanced grayscale image. This transformation converts the continuous intensity values into a binary format, simplifying the structure for edge detection and contour extraction using the thresholding strategy.

Specifically, Contrast Limited Adaptive Histogram Equalization (CLAHE) is applied at each pyramid level to enhance image contrast, particularly in low-light or low-contrast regions. To achieve that, CLAHE divides the image into small tiles (e.g., 8×8 or 16×16 pixels) and performs histogram equalization within each tile to improve feature visibility. The histogram is clipped at a threshold T to prevent noise amplification, ensuring that only meaningful contrast variations are emphasized. The enhanced intensity value C_i for a pixel is calculated using:

$$C_i = min\left(\frac{H_i}{T}, 1\right) \cdot H_i \quad (9)$$

where H_i represents the local histogram count for intensity i. This formulation ensures that histogram values exceeding T are clipped, preventing over-amplification of noise in homogeneous regions such as uniform backgrounds. Consequently, CLAHE enhances meaningful contrast variations associated with microplastic features while suppressing background noise.

For this study, CLAHE was applied using clipLimit = 3.0 and tileGridSize = 8×8, and then the threshold was determined using Otsu's method to generate a binary image. A mask was subsequently applied to exclude large circular objects (e.g., Petri dishes), thereby improving the visibility of microplastics. An example of the resulting enhancement and binarization outcome is shown in Figure 4.

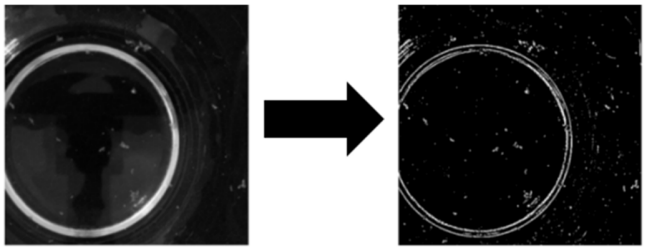

Fig. 4. Example of CLAHE enhancement at the best level.

E. Object Classification and Localization

Following CLAHE, sliding windows analysis using a 32×32 pixel size was systematically applied to the input image step-by-step, scanning each windowed region by shifting across it. This technique ensures that the detection process covers the entire image, capturing potential microplastic particles that may not be prominent on the global image scale. The implementation of sliding windows is illustrated in Figure 5.

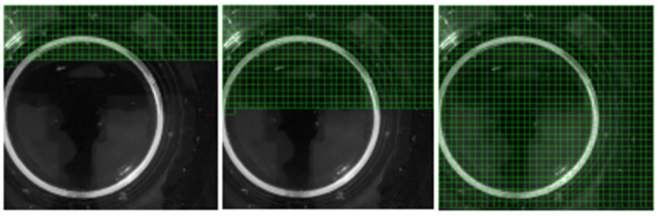

Fig. 5. Example of sliding windows analysis in images.

III. EXPERIMENTAL RESULTS AND DISCUSSION

The experimental evaluation assessed the effectiveness of the proposed adaptive Gaussian-Laplacian pyramid for microplastic detection at each pyramid level (1, 2, 3, 4, and 5) and at three different radius configurations (5, 10, and 15 pixels). Radius corresponds to the neighborhood size in the sliding window detection stage.

Performance is evaluated using accuracy, precision, recall, F1-score, and detection density (average detected objects per image) to analyze the trade-off between detection sensitivity and over-segmentation. The results are presented in Table II and Figure 6, while a representative example of microplastics detection is shown in Figure 7.

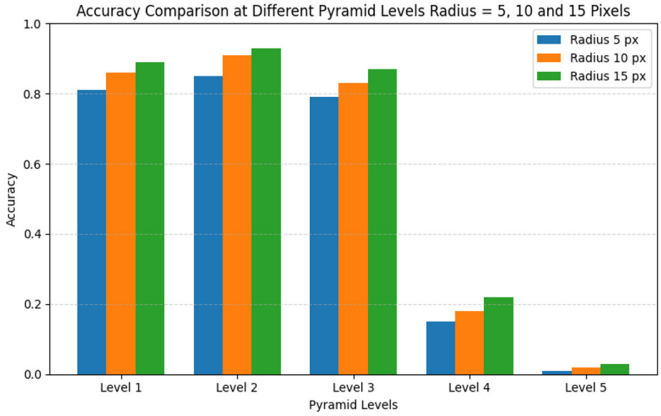

Fig. 6. Detection accuracy across pyramid levels for different radii.

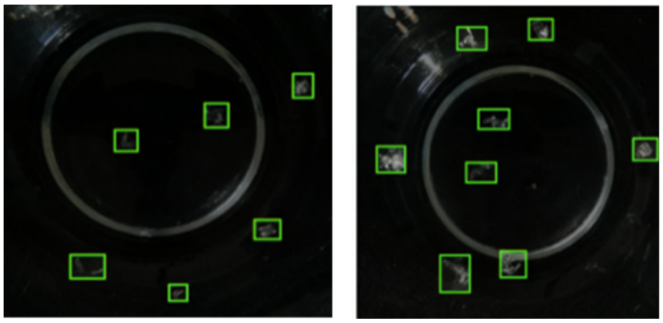

Fig. 7. Example of microplastic detection result.

As shown in Figure 6 and Table II, detection accuracy does not increase monotonically with increasing radius across pyramid levels. The highest accuracy is achieved at Level 2 with a radius of 15 pixels (0.93), while maintaining a detection density of 48.70, resulting in a more balanced overall performance with a precision of 0.92, recall of 0.89, and F1-score of 0.91. Although this setting results in a slightly lower detection density compared to a smaller radius, it provides more reliable and robust detections, as reflected by its higher precision (0.92), recall (0.89), and F1-score (0.91); thus, it is considered the best-performing configuration.

On the other hand, as shown in Table II, it is observed that pyramid Levels 4 and 5 exhibit very low performance across all radius values. This behavior is primarily caused by excessive spatial downsampling at higher pyramid levels, which significantly reduces image resolution and suppresses fine-grained edge and texture information essential for detecting small microplastic particles. As a result, many microplastic instances are no longer adequately represented and detected.

A confusion matrix for the best-performing configuration is also presented in Figure 8 based on the total of 1,171 microplastic instances. The proposed method correctly identified 414 true positive microplastic instances, with only 46 false negatives and 36 false positives.

TABLE II. PERFORMANCE METRICS AND DETECTION DENSITY ACROSS ALL PYRAMID LEVELS AND RADII

Level	Radius (pixel)	Accuracy	Precision	Recall	F1-score	Avg. Objects/Image
1	5	0.81	0.83	0.78	0.80	62.30
	10	0.86	0.87	0.84	0.85	58.10
	15	0.89	0.90	0.87	0.88	51.20
2	5	0.85	0.86	0.83	0.84	56.80
	10	0.91	0.91	0.90	0.90	55.16
	15	0.93	0.92	0.89	0.91	48.70
3	5	0.79	0.81	0.76	0.78	53.40
	10	0.83	0.85	0.80	0.82	49.60
	15	0.87	0.88	0.85	0.86	44.20
4	5	0.15	0.16	0.13	0.14	12.30
	10	0.18	0.17	0.20	0.18	8.50
	15	0.22	0.20	0.20	0.22	5.90
5	5	0.01	0.04	0.02	0.03	1.20
	10	0.02	0.03	0.01	0.02	0.80
	15	0.03	0.02	0.01	0.01	0.40

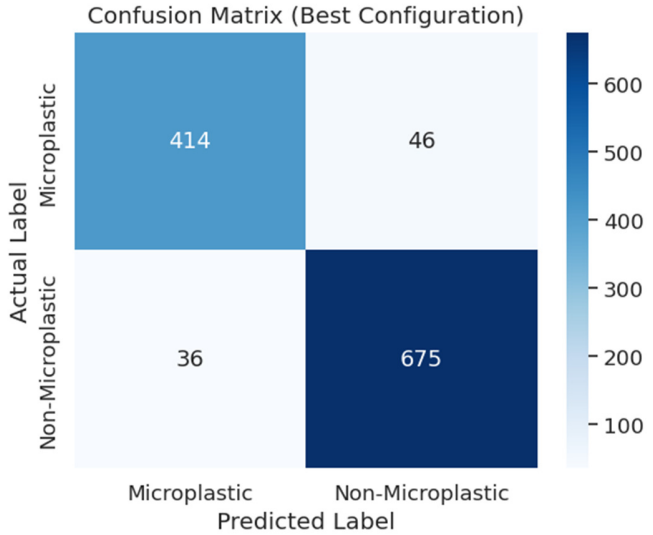

Fig. 8. Confusion matrix of the best configuration.

A. *Comparative Analysis*

Table III presents a comparative analysis of the proposed model best performing configuration against representative detection approaches, evaluated under the same microplastic dataset and experimental protocol.

TABLE III. COMPARATIVE ANALYSIS WITH REPRESENTATIVE DETECTION APPROACHES

Method	Precision	Recall	F1-score	Accuracy
Proposed method	0.92	0.89	0.91	0.93
CNN-based Methods [18]	0.88	0.85	0.86	0.88
YOLO-based Methods [19]	0.95	0.93	0.94	0.94
Multi-Scale Feature Extraction [20]	0.89	0.84	0.86	0.87
Adaptive Scale Selection [21]	0.91	0.87	0.89	0.89
Adaptive Multi-Scale Fusion [22]	0.93	0.86	0.89	0.89

Although YOLO-based methods [19] achieved the highest accuracy (0.94) and F1-score (0.94), this framework requires large, annotated datasets and substantial computational resources. In contrast, the proposed method achieved competitive performance without deep learning training, making it more suitable for data- and resource-limited scenarios. Traditional CNN-based [18] and classical multi-scale approaches [20-22] showed lower performance on the same dataset, mainly due to the absence of explicit texture-enhancement mechanisms for microplastic detection.

IV. CONCLUSION

The adaptive Gaussian-Laplacian pyramid has proven to be an effective technique for multi-scale image decomposition in microplastic detection. This method enhances the detection of microplastic particles with varying shapes and textures by dynamically selecting the optimal pyramid level based on metrics such as variance, edge energy, and entropy. By integrating adaptive level selection, contrast enhancement, and robust feature extraction, the method provides a flexible framework suitable for real-world applications.

Despite the promising results, the study has limitations. Further validation on larger and more diverse datasets is required to ensure generalizability and robustness. Additionally, expanding the range of environmental conditions and microplastic types represented in the ground truth data will help refine model performance and strengthen its applicability to large-scale environmental monitoring systems.

ACKNOWLEDGMENT

This work was supported by the Final Project Research Grant for the Master of Computer Science, Department of Computer Science and Electronics, Faculty of Mathematics and Natural Sciences, Universitas Gadjah Mada, Indonesia, with Contract Number 4496/UN1/FMIPA.1.3/KP/PT.01.03/2025.

REFERENCES

[1] M. N. Issac and B. Kandasubramanian, "Effect of microplastics in water and aquatic systems," *Environmental Science and Pollution Research*, vol. 28, no. 16, pp. 19544–19562, Apr. 2021, https://doi.org/10.1007/s11356-021-13184-2.

[2] X. Sun and X.-F. Sun, "An edge detection algorithm based upon the adaptive multi-directional anisotropic Gaussian filter and its

applications," *The Journal of Supercomputing*, vol. 80, no. 11, pp. 15183–15214, July 2024, https://doi.org/10.1007/s11227-024-06044-6.

[3] A. H. Anik, S. Hossain, M. Alam, M. Binte Sultan, Md. T. Hasnine, and Md. M. Rahman, "Microplastics pollution: A comprehensive review on the sources, fates, effects, and potential remediation," *Environmental Nanotechnology, Monitoring & Management*, vol. 16, Dec. 2021, Art. no. 100530, https://doi.org/10.1016/j.enmm.2021.100530.

[4] V. Asha, G. M, M. L. Kolambkar, M. P, N. G. V, and A. Prasad, "Classification of Plastic Waste Products using Deep Learning," in *2024 1st International Conference on Cognitive, Green and Ubiquitous Computing (IC-CGU)*, Bhubaneswar, India, Mar. 2024, pp. 1–6, https://doi.org/10.1109/IC-CGU58078.2024.10530692.

[5] G. Abbas, U. Ahmed, and M. A. Ahmad, "Impact of Microplastics on Human Health: Risks, Diseases, and Affected Body Systems," *Microplastics*, vol. 4, no. 2, May 2025, Art. no. 23, https://doi.org/10.3390/microplastics4020023.

[6] S. Matavos-Aramyan, "Addressing the microplastic crisis: A multifaceted approach to removal and regulation," *Environmental Advances*, vol. 17, Oct. 2024, Art. no. 100579, https://doi.org/10.1016/j.envadv.2024.100579.

[7] M. E. Mihailov, A. V. Chiroșca, E. D. Pantea, and G. Chiroșca, "Machine Learning Approaches for Microplastic Pollution Analysis in Mytilus galloprovincialis in the Western Black Sea," *Sustainability*, vol. 17, no. 12, June 2025, Art. no. 5664, https://doi.org/10.3390/su17125664.

[8] P. Akkajit, M. E. E. Alahi, and A. Sukkuea, "Enhanced detection and classification of microplastics in marine environments using deep learning," *Regional Studies in Marine Science*, vol. 80, Dec. 2024, Art. no. 103880, https://doi.org/10.1016/j.rsma.2024.103880.

[9] Y. Yao, W. Xu, and H. Fan, "A Deep Learning Approach for Microplastic Segmentation in Microscopic Images," *Toxics*, vol. 13, no. 12, Nov. 2025, Art. no. 1018, https://doi.org/10.3390/toxics13121018.

[10] T. Saidani, "Deep Learning Approach: YOLOv5-based Custom Object Detection," *Engineering, Technology & Applied Science Research*, vol. 13, no. 6, pp. 12158–12163, Dec. 2023, https://doi.org/10.48084/etasr.6397.

[11] K. Han et al., "Innovative methods for microplastic characterization and detection: Deep learning supported by photoacoustic imaging and automated pre-processing data," Journal of Environmental Management, vol. 359, May 2024, Art. no. 120954, https://doi.org/10.1016/j.jenvman.2024.120954.

[12] T. Tanprawat, S. Laitrakun, P. Somnuake, and P. Opaprakasit, "Microplastic Spectral Classification Using Deep Learning with Denoising and Dimensionality Reduction," in *2024 9th International Conference on Business and Industrial Research (ICBIR)*, Bangkok, Thailand, May 2024, pp. 0811–0816, https://doi.org/10.1109/ICBIR61386.2024.10875756.

[13] S. Sundar, "A Novel Low-Cost Approach For Detection, Classification, and Quantification of Microplastic Pollution in Freshwater Ecosystems using IoT devices and Instance Segmentation," in *2022 IEEE MIT Undergraduate Research Technology Conference (URTC)*, Cambridge, MA, USA, Sept. 2022, pp. 1–5, https://doi.org/10.1109/URTC56832.2022.10002222.

[14] L. Wei, "Genetic Algorithm Optimization of Concrete Frame Structure Based on Improved Random Forest," in *2023 International Conference on Electronics and Devices, Computational Science (ICEDCS)*, Marseille, France, Sept. 2023, pp. 249–253, https://doi.org/10.1109/ICEDCS60513.2023.00051.

[15] Z. Chen *et al.*, "A Hybrid MIR-spectrum Processing Algorithm for Microplastics Analysis," in *2024 7th International Conference on Electronics Technology (ICET)*, Chengdu, China, May 2024, pp. 1120–1125, https://doi.org/10.1109/ICET61945.2024.10672915.

[16] *Microplastic Dataset Computer Vision Dataset*. (2022), Panats MP Project. [Online]. Available: https://universe.roboflow.com/panats-mp-project/microplastic-dataset.

[17] M. M. Nanavati and M. Shah, "Implementation and Comparative Study of Pyramid-based Image Fusion Techniques for Lumbar Spine Images," *Engineering, Technology & Applied Science Research*, vol. 13, no. 4, pp. 11139–11145, Aug. 2023, https://doi.org/10.48084/etasr.5960.

[18] S. Galata, I. Walkington, T. Lane, K. Kiriakoulakis, and J. J. Dick, "Rapid detection of microfibres in environmental samples using open-source visual recognition models," *Journal of Hazardous Materials*, vol. 480, Dec. 2024, Art. no. 135956, https://doi.org/10.1016/j.jhazmat.2024.135956.

[19] M. Z. Bin Zahir Arju *et al.*, "Deep-learning enabled rapid and low-cost detection of microplastics in consumer products following on-site extraction and image processing," *RSC Advances*, vol. 15, no. 14, pp. 10473–10483, 2025, https://doi.org/10.1039/D4RA07991D.

[20] X. Yu, S. Wu, X. Lu, and G. Gao, "Adaptive multiscale feature for object detection," *Neurocomputing*, vol. 449, pp. 146–158, Aug. 2021, https://doi.org/10.1016/j.neucom.2021.04.002.

[21] J. Zhang *et al.*, "Small object intelligent detection method based on adaptive recursive feature pyramid," *Heliyon*, vol. 9, no. 7, July 2023, Art. no. e17730, https://doi.org/10.1016/j.heliyon.2023.e17730.

[22] G. Wen, L. Cheng, H. Yuan, and X. Li, "Surface Defect Detection Based on Adaptive Multi-Scale Feature Fusion," *Sensors*, vol. 25, no. 6, Mar. 2025, Art. no. 1720, https://doi.org/10.3390/s25061720.